Geometric considerations of the monoclinic–rutile structural transition in VO2

Shian Guan, Aline Rougier, Matthew R. Suchomel, Nicolas Penin, Kadiali Bodiang, Manuel Gaudon

Dalton Transactions

ARTICLE

Received 00th January 20xx,
Accepted 00th January 20xx

DOI: 10.1039/x0xx00000x

www.rsc.org/

Geometric considerations of the monoclinic - rutile structural transition in VO_2

Shian Guan, Aline Rougier, Matthew R. Suchomel, Nicolas Penin, Kadiali Bodiang and Manuel Gaudon

The mechanism of the displacive phase transition in VO_2 near the transition temperature is discussed in terms of a geometrical approach, combining simple calculations based on the Brown's band valence model and *in situ* X-ray diffraction experimental results. Considering that the structural origin is well linked to the electrostatic potential optimization as in a Peierls model, our geometrical calculations and experimental studies are in agreement and suggest that VO_2 phase transition is the consequence of very short atomic shifts mainly associated to a decrease of the 2nd sphere coulombic interactions. Hence, at a given temperature, the allotropic form (monoclinic versus rutile form) offering the largest unit-cell volume is stabilized over the lower unit-cell volume allotropic, while the transition occurs at the intercept of the unit cell variation versus temperature of the two forms, which exhibit significantly different thermal expansion coefficients.

Introduction

The origin of the driving force(s) behind the metal-insulator transition (MIT) of VO_2 has been the subject of controversy for decades. Structurally, the MIT transition at approximately 70 °C is accompanied by a change from a high-temperature tetragonal rutile structure (S.G. *P*42/*mnm*) to a low-temperature monoclinic (M) form (S.G. *P*21/*c*) characterized by a structural twist and V^{4+} cations shift along the rutile *c* axis to form V-V pairs (homopolar bonds) [1]. From a simplistic point of view considering the orthonormal referential constituted by the octahedral cage edges, the key aspect of the transition is an off-centring of vanadium ions along (111), with an antiferroelastic correlation. A crystal description of the transition was first reported by Goodenough *et al.* [2], associating the lattice distortion (pairing and tilting) in the VO_2 (M) phase with an increase of the antibonding 3*d* band above the Fermi level. Herein lies the controversial point; whether the phase transition originates from the crystal distortion and unit-cell doubling (Peierls mechanism), or from the opening of a correlation gap due to the presence of electron-electron correlations (Mott mechanism) [3].

Recent structural calculations (Peierls approach) based on density functional theory within the local density approximation tends to predict the monoclinic phase as the most stable [4-9]. In a complex structural approach, i.e. using the Buckingham potential to describe the short-range interaction (V-O and O-O bonds), a Morse potential for V-V interaction (at the origin of the octahedral chain distortion) and additional optimization techniques, Woodley [10] concludes that monoclinic and rutile free energies cross at nearly 300K, in favour of a Peierls transition. Cavalleri *et al*. [11] showed evidence of a structurally driven transition with the use of ultrafast pump-probe spectroscopy. Conversely, several authors argue for a Mott-driven transition [12-14] based on experimental parameters such as switching time using femto-laser sources [12,13] or by measuring the electromagnetic response of a VO_2 thin film by scattering scanning near-field infrared microscopy. [14] Current interpretations seem to propose a combination of both mechanisms simultaneously; meanwhile the appearance of new phases during the structural phase transition (well supported by nanoscale imaging techniques and/or optical/electronic spectroscopy) makes it increasingly critical to understand the true nature of this transition [15-19]. Despite the complex nature of previously reported theoretical structure calculations, a basic interpretation of the transition in terms of fundamental geometrical factors such as unit-cell volume and bond distances is often neglected in these studies. However, these parameters are linked to the thermal expansion and coulombic interactions of both VO_2 allotropic forms and are thus potential significant driving forces to consider near the boundary of the structural transition.

Within the limit of a simple geometrical approach, we describe here a new approach for evaluating the main driving forces involved in the MIT transition of VO_2. This approach compares measured unit-cell parameters to basic calculations for the cell volume and electrostatic potential of the 1st and 2nd sphere anion/cation pairs in monoclinic and rutile structure types near the phase transition. Calculations are based on the well-established bond valence model, [20] and can be rapidly performed with a standard spreadsheet software package. The experimental temperature dependence of monoclinic and rutile phase unit-cell parameters near the transition temperature for this study were obtained from *in-situ* synchrotron powder diffraction measurements of VO_2 samples, the synthesis of which was previously reported. [21]

Calculations

Using Brown's bond valence model [20] to evaluate all atom positions in a structural unit cell with a basic set of geometric

[a] CNRS, Univ. Bordeaux, Bordeaux INP, ICMCB, UMR 5026, F-33600 Pessac, France

equations is a powerful tool which has been previously used with success to predict crystal structure anisotropy (as in Würtzite compounds [22]) or even multiple phase transitions (as in the $BaTiO_3$ perovskite [23]). In this type of an approach, atomic positions are typically relaxed to minimize the electrostatic potential between first neighbouring cations and anions pairs. The constraints of the Brown equations result in convergence towards a single solution, i.e. the valence of the vanadium ion deduced from the bond valence model must be kept equal to 4. For the binary ionic compound as VO_2, the Brown equation for each V-O pair relating bond lengths and bond valences is thus BV = $\exp[(r_0 - d_{ij})/0.37]$ with BV: bond valence, r_0 = 1.78 Å (V-O bond empirical parameter given by Brown tables) and d_{ij} = V-O bond length in Å. In the VO_2 crystal structure, as the vanadium cations occupies an octahedral coordination site, six bonds are summed up for the valence of the vanadium cations.

The initial step of this geometrical approach was to consider positional shifts of vanadium ions in the octahedral cages of the rutile (tetragonal) vs. monoclinic structures and to examine if V^{4+} decentring is associated with an increase of the surrounding 1st sphere coulombic interaction E(1st sphere) (*i. e.*, a stabilization effect) and thus connected to the transition between these polymorphic forms. The parameters used to describe the rutile structure are shown in **Fig. 1*a*** and ***c***, the unit-cell parameters; *x*, describing the oxygen position at (x, x, 0); *l'*, the edge length of the octahedral cages along the octahedral chains; *l''*, the shared edge length of the octahedral chains; and h, the half-height of the octahedral cage (note that *h* is identical to the distance of apical V-O bonds, while the other 4 equivalent equatorial V-O bonds are noted as *r* in **Fig. 1**). The equations linking these parameters are: $h = \sqrt{2}.a.x$; $r = [(\frac{1}{2}.l')^2 + (\frac{1}{2}.l'')^2]^{\frac{1}{2}}$; $l' = c$; $l'' = 2.\sqrt{2}.(0.5 - x)$ and $V_{cell} = a^2.c$. Considering an ionic approach, the first sphere potential is defined as E(1st sphere) = $K.(2/h + 4/r)$, where K is a constant.

A simplified geometric description of the pseudo-monoclinic VO_2 structure can be obtained by considering only V^{4+} decentring along [111] direction as oxygen site displacements in the distorted octahedral cages are negligible.

This leads to the new set of equations: δ is the amplitude of the decentring in (111) direction; α is the angle of the [111] axis with respect to the equatorial plane of the octahedral cage; $h' = (h^2 + \delta^2 - 2.h.\delta''.\sin\alpha)^{\frac{1}{2}}$; $h'' = (h^2 + \delta^2 + 2.h.\delta''.\sin\alpha)^{\frac{1}{2}}$; $r' = [(\frac{1}{2}l')^2 + (\frac{1}{2}l'')^2 + \delta^2 - \delta.l'.\cos\alpha]^{\frac{1}{2}}$; $r'' = [(\frac{1}{2}l')^2 + (\frac{1}{2}l'')^2 + \delta^2 + \delta.l'.\cos\alpha]^{\frac{1}{2}}$; $l' = c$; $l'' = 2\sqrt{2}(0.5 - x)$; $V_{cell} = a^2.c$. The first sphere potential becomes E (1st sphere) = $K.(1/h' + 1/h'' + 2/r' + 2/r'')$. *c*, *a* and x as have been considered as variables in order to maximize (considering positive terms for crystal energies) the E (1st sphere) versus δ. From these calculation, E (1st sphere) and the optimised unit cell volume can be plotted versus cation decentering (**Fig. 2**).

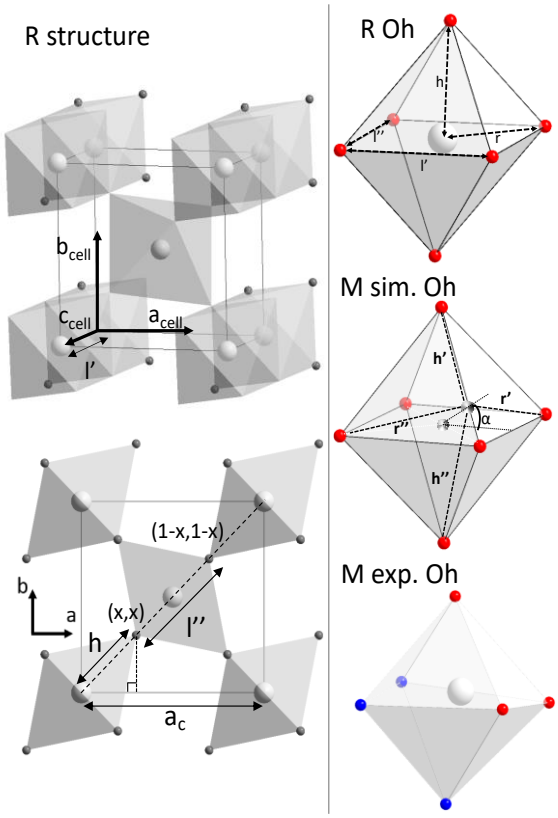

Figure 1: Rutile VO_2 structure with l' and l'' are the two edges lengths of the octahedral equatorial rectangle, h the half height of the octahedron, and oxygen in (*x*, *x*, 0) Wyckoff position. Vanadium octahedral sites and their associated parameters in rutile, monoclinic or "simulated" monoclinic structure: *i.e.* considering a rutile octahedral cage with a cation δ decentring in (111) direction. (r' and r'' represent two V-O bonds distance in the plane after V^{4+} decentring)

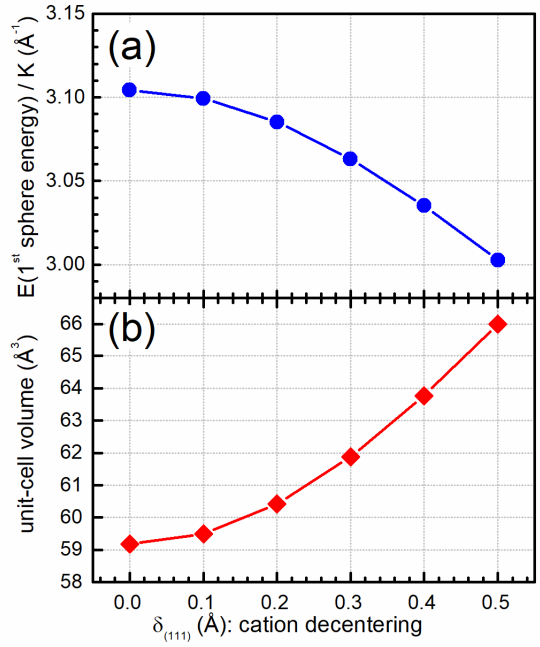

Figure 2: Effect of the consideration of δ decentring amplitude in the simulated monoclinic structure on the electrostatic potential (1st sphere energy) (a) and the unit-cell volume (b).

As shown in **Fig. 2a**, the decrease of E(1stsphere) with δ shows that our ionic approach fails to explain the rutile to monoclinic phase transformation. With a higher absolute energy, the tetragonal environment appears most stable in these geometrical calculations, with any monoclinic-type decentring (δ) appears to reduce the overall energy. However, based on the same calculations, it is noted that the unit-cell volume is predicted to slightly increase with vanadium cation decentring (**Fig. 2b**), suggesting that the transition may be eased by an expansion of the cell volume. This later result is somewhat unexpected, as crystal energies are normally to increase (stability increase) with crystal density (i.e. with shortening bond lengths).

In a second step, the origin of the tetragonal distortion is evaluated, *i.e.* the E(1st sphere) and unit-cell volume of tetragonal phase are calculated versus the *c/a* ratio. The goal of this analysis is to probe why the VO_2 rutile phase does not exhibit cubic symmetry; a discussion that could in principle be extended to all rutile compounds typically exhibiting a tetragonal distortion. The isotropic point, defined by a *c/a* ratio equal to 0.586 (*i.e.* $\sqrt{2}.(\sqrt{2}-1)$), corresponds to a "cubic-rutile form". For the calculation, the *c/a* value is fixed while *a* and *x* are variables adjusted in order to minimize the E(1st sphere). Regardless of the tetragonal distortion a stable minimum for the E(1st sphere) can be determined (**Fig. 3a**). Despite the tetragonal distortion of the unit-cell and consequently of the octahedral cages also, the six V-O bond lengths remain constant. Indeed, the distortion of the equatorial plane of the octahedral site can be followed via the evolution of the *l'* and *l''* parameters (**Fig. 3c**), but this distortion occurs such as the *r* bond lengths remain equal to the *h* length, whatever the *c/a* ratio (fixed refined values for *r* = *h* = 1.930 Å). Thus, the tetragonal distortion from the cubic form of the rutile structure is apparently not due to a minimization of the E(1st sphere). In addition, it is noted that the plot of unit-cell volume versus *c/a* adopts a bell-shape curve with a maximum at approximately *c/a* ≈ 0.626 (**Fig. 3b**), in good agreement with experimental measured values for the rutile form of VO_2. Moreover, by fixing *ab initio* the value of *h* to 1.930 Å, since no deviation of this parameter was found with varying *c/a* ratio, it is possible to treat all *a*, *c* (and so *c/a*) and *x* parameters as variables, and to perform a calculation in order to maximize the unit-cell volume. This optimization leads to a crystal defined by a *c/a* ratio of 0.626, with *a* = 5.754 Å, *c* = 2.870 Å, with characteristic octahedral lengths of *l'* = 2.87 Å, *l''* = 2.57 Å and *r* = *h* = 1.93 Å. Interestingly, these calculated lengths are very similar to the experimental parameters given in the literature for VO_2 (R) phase [24-27]. The stability of the rutile form is therefore strongly linked to a maximization of the cell volume while simultaneously maintaining the E(1st sphere). Indeed, the cell volume maximization is directly correlated to the minimization of the E(2nd sphere), *i.e.* the decrease of the anion-anion or cation-cation coulombic repulsions. Moreover, these conclusions are supported by an additional calculation performed to minimize the E(2nd sphere) using the set of shortest V-V and O-O bond lengths. In a manner analogous to

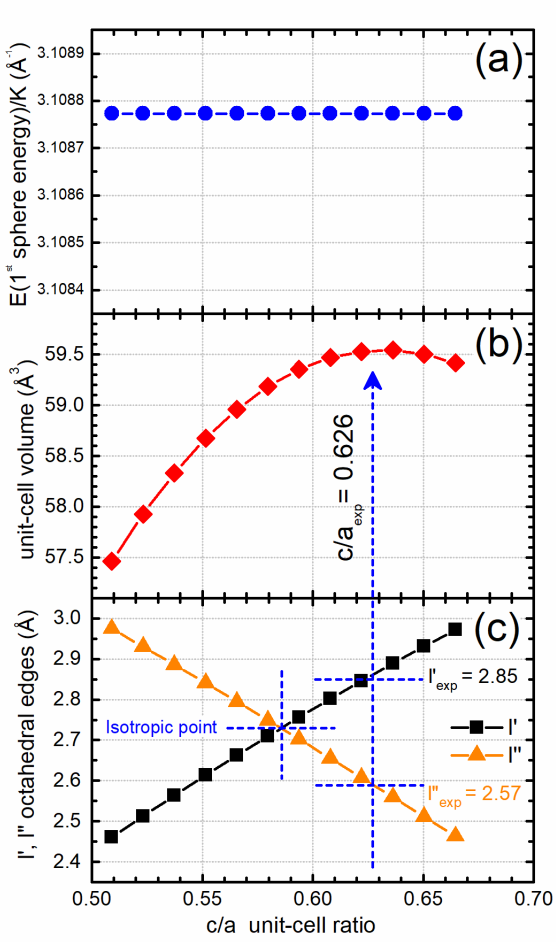

Figure 3: Effect of the *c/a* tetragonal distortion on the electrostatic potential (1st sphere energy) (a); the unit-cell volume (b) and the *l'* and *l''* octahedral edges lengths (c).

that detailed above, the bond distances can be described as follows: 2 V-V bonds and the 2 O-O bonds = 2.*l'*, the 8 V-V bonds = $[(h + ½.l'')^2 + (½.l')^2]^{1/2}$, the 8 O-O bonds = $(h^2 + r^2)^{1/2}$ + 2.*l'*, the 2 last O-O bonds = $[(2.x.a)^2 + (a - 2.x.a)^2]^{1/2}$. Then the E(2nd sphere) minimization calculations are performed with *a*, *c* and *x* as variables, and *h* fixed to 1.93 Å (as above), the overall crystal parameters results are nearly identical to that found with the described cell volume maximization calculations.

Hence our basic geometric calculation clearly shows that by considering only a Peierls origin for the VO_2 phase transition, with a pure ionic bond approach, the tetragonal distortion of the rutile phase is well explained by an energy minimization. The tetragonal distortion allows the decrease of the crystal energy which can be approximated as E(crystal) = E(1st sphere) - E(2nd sphere). The originality of the system is that the tetragonal distortion does not impact of E(1st sphere); thus, the optimization of the electrostatic potential is governed by E(2nd sphere) associated with cell volume maximization. This result on the driving forces of the tetragonal distortion origin has to be correlated to our first calculation showing that the monoclinic to rutile phase transition is not associated with an increase of the cation-anion interaction potential (1st sphere maximization) but may be promoted by an increase in the unit cell volume (2nd sphere minimization).

Experimental Results

Synthesis details of the VO_2 (M) powder, which showed minor trace of a V_3O_7 impurity, has been described previously [1]. The phase transition as a function of temperature was followed by *in-situ* powder diffraction. High-resolution synchrotron X-ray powder diffraction (HR-SPD) data of VO_2 have been recorded on both heating and cooling with 20 °C temperature steps between 280 and 380 °C using beamline 11-BM at the Advanced Photon Source (APS), Argonne National Laboratory. For each temperature scan, data were collected over a 0.5-35° 2θ range with a 0.001° step size using a wavelength of λ = 0.41417 Å; the powder sample being sealed in a 0.8 mm diameter Kapton capillary and was spun at 60 Hz during data collection (**Fig. 4a**). Determination of VO_2 unit cell

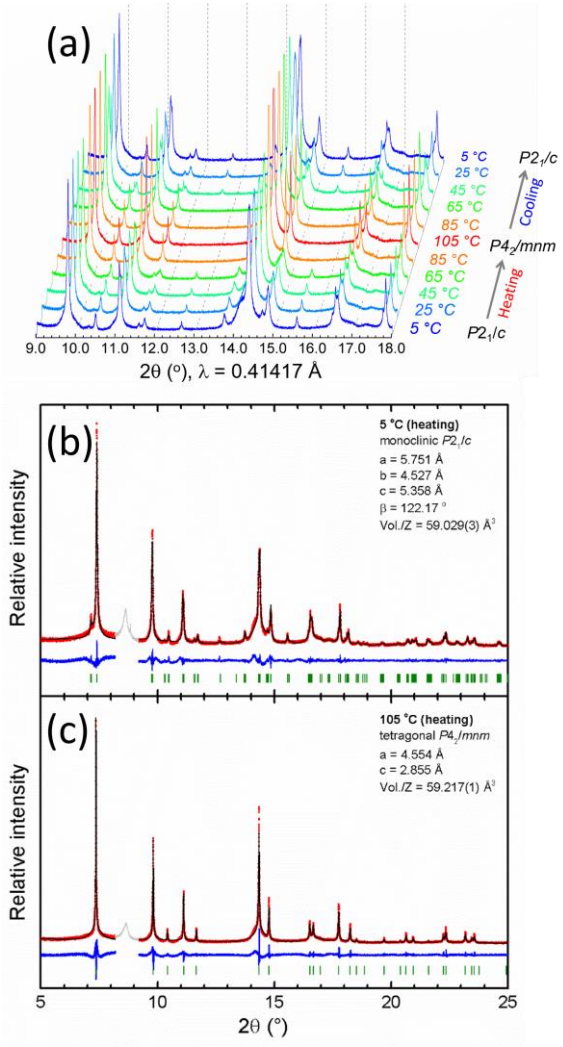

Figure 4: Synchrotron powder diffraction pattern over the 5°C→105°C temperature range showing the reversible transition between monoclinic phase ($P2_1/c$) and rutile ($P4_2/mnm$) structures on heating and cooling (a). Profile fits of VO_2 HR-SPD data collected at 5 °C (b) and 105 °C (c), showing the observed (red points) and calculated (black line) intensities as a function of 2θ angle. The difference profile and unit cell *hkl* reflections are shown below as a blue line and green ticks, respectively. The exclude 2θ region (approximately 8 - 9°) is indicated by light grey data points.

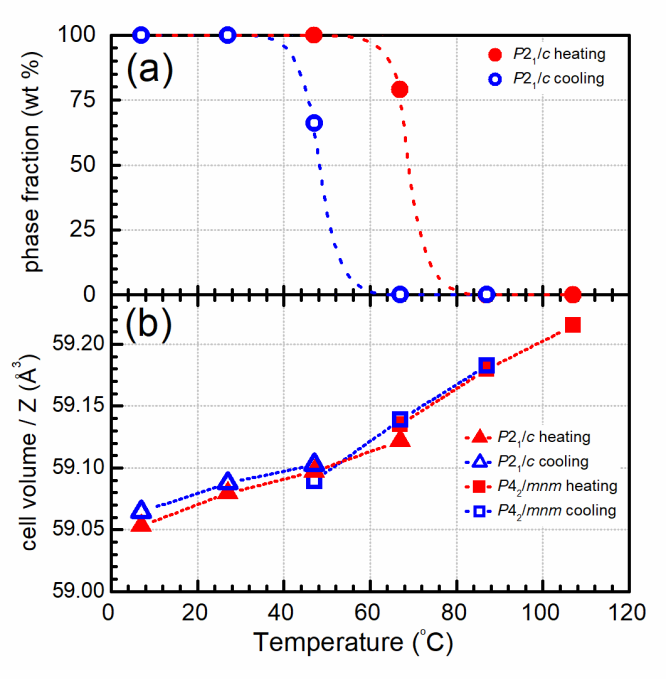

Figure 2: (a) Phase fraction (weight %) of the monoclinic phase as a function of temperature on heating and cooling, (b) VO_2 unit cell volume (per formula unit Z) as a function of temperature on heating and cooling.

parameters were performed by profile matching and cell fractions from Rietveld refinements using the TOPAS software package, as illustrated on the low (monoclinic) and the high (tetragonal) temperature forms recorded at 5°C (**Fig. 4b**) and 105°C (**Fig. 4c**), respectively.

The evolution of the rutile and monoclinic phase fractions over the studied temperature range are summarized in **Fig. 5a**. The unit-cell parameters of both rutile and monoclinic forms were refined, and normalized unit cell volumes *vs*. temperature are plotted to support the discussion (**Fig. 5b**). The rutile to monoclinic phase transition is described by a hysteresis loop, centred on 65-70 °C with a width of about 20°C : it can be seen that at 65°C the percentage of rutile phase / monoclinic phase ratio in the heating mode is about the same than the one calculated at 45°C in the cooling mode. in good agreement with past studies [2, 12-19]. The evolution of both cell parameters versus temperature shows that the volumetric coefficients of thermal expansion for the two phases are significantly different. Using a simple linear slope fit of the low temperature (monoclinic) and high temperature (tetragonal) unit cell volumes, we can estimate the volumetric thermal expansion coefficients ($\alpha_{Vol.}$) using $\alpha_{Vol.} = (\Delta V/\Delta T)/V$, where $\Delta V/\Delta T$ is simply the linear fit slope. For the low temperature (monoclinic) phase, $\alpha_{Vol.} = 20.3 \times 10^{-6}\ K^{-1}$ and for high temperature (tetragonal) phase, $\alpha_{Vol.} = 37.2 \times 10^{-6}\ K^{-1}$. Note that for ideal anisotropic materials, the $\alpha_{vol.}$ value is 3 times larger than the linear thermal expansion coefficient; these estimated volumetric thermal expansion coefficients are in good agreement with the range of VO_2 literature values [28].

The rutile form exhibits a higher α_{Vol} than the monoclinic one. On the transition temperature, the volume of the two

phases is similar, *i.e*. the intersection point of the unit-cell evolution is located at the transition temperature. Consequently, due to the hysteresis phenomenon linked to the 1st order character of the phase transition, and due to the mismatch between the monoclinic thermal expansion coefficient (TEC) and the rutile TEC, both in cooling and heating modes, the transition is associated with a slight volume expansion. The volume expansion is experimentally with an amplitude of about 0.01 Å^3 in cooling mode: measured between the monoclinic (blue triangle) and rutile phase (blue square) at 45°C, and about 0.02 Å^3 in the heating mode: measured between the monoclinic (blue triangle) and rutile phase (blue square) at 45°C. Thus, the volume expansion in both heating and cooling mode produced by the phase transition is roughly 0.025% volume (or 0.3% of bond length variation). It is apparently a minor change, but it well governs the phase transition. The stable form is the one with the highest unit-cell volume (per formula unit Z). Such a transition scheme is very different to most other 1st order transitions in crystalline solids for which the volume difference between the two crystalline forms around the transition is the main aspect (as in the textbook austenite-martensitic example [29-30] or for the AMO_4 phase transitions [31-33]). From these experiments, it appears that the driving force of the transition comes from this volume difference: a greater unit-cell volume leads to higher crystal structure stability.

Conclusion

This work considers the advantage of simplistic geometric examination of the much studied VO_2 transition, in a marked contrast to the very complex literature debates on competing Peierls and Mott-type origins. From a solid-state chemistry point of view, there is often considerable benefit to interpret such transitions in terms of a structural origin and an optimization of electrostatic potentials. Through the positively correlated calculations and experimental data examined in this work, it is shown that the VO_2 rutile to monoclinic phase transition is likely the consequence of very short atomic shifts, leading to non-significant (at least non-dominant) changes on the charge interactions of the cations and anions in first neighbouring, however allowing a decrease of the 2nd sphere coulombic interactions.

Conflicts of interest

There are no conflicts to declare.

Acknowledgements

Use of the Advanced Photon Source at Argonne National Laboratory was supported by the U. S. Department of Energy, Office of Science, Office of Basic Energy Sciences, under Contract No. DE-AC02-06CH11357.

References

1 F.J. Morin, *Physical Review Letters*, 1959, **3**, 34.

2 J.B. Goodenough, *Journal of Solid State Chemistry*, 1971**,** **3**, 490.

3 A. Zylbersztejn and N.F. Mott, *Physical Review B*, 1975, **11**, 4383.

4 J.M. Booth and P.S. Casey, *Physical Review Letters*, 2009, **103**, 086402.

5 C. Sun, L. Yan, B. Yue, H.Liu and Y. Gao, Journal of Materials Chemistry C, 2014, **2**, 9283.

6 R.M. Wentzcovitch, W.W. Schulz and P.B. Allen, *Physical Review Letters*, 1994, **72**, 3043.

7 R.M. Wentzcovitch, W.W. Schulz and P.B. Allen, *Physical Review Letters*, 1994, **72**, 3389..

8 J. Shi, R. Bruinsma and A.R. Bishop, *Synthetic Metals*, 1991, **41**, 3527.

9 V. Eyert, *Annalen der Physik*, 2002, **11**, 650.

10 S.M. Woodley, *Chemical Physics Letters*, 2008, **453**, 167.

11 A. Cavalleri, T. Dekorsy, H.H.W. Wong, J.C. Kieffer and R.W. Schoelein, *Physical Review B*, 2004, **70**, 161102.

12 M.F. Becker, A.B. Buckman, R.M. Walser, T. Lepine, P. Georges and A. Brun, *Applied Physical Letters*, 1994, **65**, 1507.

13 H.T. Kim, B.D. Chae, D.H. Youn, S.L. Maeng and K.Y. Kang, *New Journal of Physics*, 2004, **6**, 52.

14 M.M. Qazilbash, M. Brehm, B.G. Chae, P.C. Ho, G. O. Andreev, B. J. Kim, S. J. Yun, A. V. Balatsky, M. P. Maple, F. Keilmann, H. T. Kim and D. N. Basov, *Science*, 2007, **318**, 1750.

15 P. Baum, D.S. Yang and A.H. Zewail, *Science*, 2007, **318**, 788.

16 M.W. Haverkort, Z. Hu, A. Tanaka, W.Reichelt, S.V. Streltsov, MA. A Korotin, V.I. Anisimov, H.H. Hsieh, H.J. Lin, C.T. Chen, D.I. Khomskii, L.H. Tjeng, *Physical Review Letters*, 2005, **95**, 196404.

17 N. Netsianda, P.E. Ngoepe, C.R.A. Catlow and S.M. Woodley, Chemistry of Materials, 2008, **20**, 1764.

18 A. Simo, K. Kaviyarasu, B. Mwakikunga, R.Madjoe, A. Gibaud and M.Maaza, *Journal of Electron Spectroscopy and Related Phenomena*, 2017, **216**, 23.

19 W. Ning, H. Yizhong, S. Magdassi, D. Mandler, L. Hai and L. Yi, *RSC Advances*, 2013, **3**, 7124.

20 I.D. Brown and D. Altermatt, *Acta Crystallographica*, 1985, **B41**, 244.

21 I. Mjejri, A. Rougier, M. Gaudon, *Inorganic Chemistry*, 2017, **56**, 1734.

22 I. Trenque, S. Mornet, A. Villesuzanne and M. Gaudon, *Solid State Science*, 2013, **21**, 81.

23 M. Gaudon, *Polyhedron*, 2015, **88**, 6.

24 M. Ghedira, H. Vincent, M. Marezio and J.C. Launay, *Journal of Solid State Chemistry*, 1977, **22**, 423.

25 D.B. McWhan, M. Marezio, J.P. Remeika and P.D. Dernier, *Physical Review B*, 1974, 10, 490.

26 S.V. Ovsyannikov, Y.G. Zainulin, N.I. Kadyrova, A.P. Tyutyunnik, A.S. Semenova, D. Kasinathan, A.A. Tsirlin, N. Miyajima and A.E. Karkin, *Inorganic Chemistry*, 2013, **52**, 11703.

27 H.R. Hoekstra, S. Siegel and F.X. Gallagher, *Advances in Chemistry Series*, 1971, **98**, 39.

28 D. Kucharszick and T. Niklewski, *Journal of Applied Crystallography*, 1979, **12**, 370.

29 B. Zhao, L. Li, F. Lu, F., Q. Zhai, B. Yang, C. Schick and Y. Gao, *Thermochimica Acta*, 2015, **603**, 2.

30 J.-C. Zhao and M.R. Notis, *Materials Science and Engineering R*, 1995, **15**, 135.

31 L. Robertson, N. Penin, V. Blanco-Gutierrez, D. Sheptyakov, A. Demourgues, M. Gaudon, *Journal of Materials Chemistry C*, 2015, **3**, 2918.

32 M. Gaudon, P. Deniard, A. Demourgues, C. Carbonera, A. Le Nestour, A. Largeteau, J.-F. Létard, S. Jobic, *Advanced Material*s, 2007, **19**, 3517.

33 L.C. Robertson, M. Gaudon, S. Jobic, P. Deniard, A. Demourgues, *Inorganic Chemistry*, 2011, **50**, 2878.